

COSMOLOGICAL CONDUCTIVE/COOLING FRONTS

AS Ly α FOREST CLOUDS

A. Ferrara¹ and Yu. Shchekinov²

¹ *Osservatorio Astrofisico di Arcetri, Largo E. Fermi, 5, 50125 Florence, Italy*

² *Institute of Physics, Rostov University, 194 Stachki, 344104 Rostov on Don, Russia*

ABSTRACT

We propose a simple model for the origin and evolution of Ly α forest clouds based on cosmological conductive/cooling fronts. In this model the Ly α forest arises in the interfaces between the IGM and cold clouds that could be tentatively identified with protogalaxies. Most of the properties of the Ly α forest absorbers are reproduced with a very restricted number of assumptions. Among these are the correct range of HI column density, cloud sizes and redshift and HI column density distributions for the absorbers. Several predictions and implications of the model are briefly discussed.

Subject Headings: intergalactic medium — quasars: absorption lines

1. Introduction

The remarkable observational progresses made in the last few years allow to tackle the problem of the origin and evolution of Ly α forest clouds in a more firm and quantitative manner. In brief, the available observational constraints that every model for the Ly α forest clouds should fulfill are the following. The typical range of hydrogen column density is $10^{12}\text{cm}^{-2} \leq N_{HI} \leq 10^{16} \text{ cm}^{-2}$ (Dobrzycki & Bechtold 1996). Doppler parameters are typically $b = 30 \text{ km s}^{-1}$, even if some claims of much smaller values of b have been made (Pettini *et al.* 1990; Carswell *et al.* 1991; Rauch *et al.* 1993; Giallongo *et al.* 1993). Lower limits on the sizes are provided by a small number of experiments using quasar pairs (Dinshaw *et al.* 1994, Bechtold *et al.* 1994) which generally agree that transverse sizes should be $\geq 100 \text{ kpc}$.

Here we propose an alternative view of the origin and evolution of Ly α forest absorbers, based on the theory of conductive/cooling fronts described by Ferrara & Shchekinov (1993) (FS93). The basic idea is that Ly α forest clouds may represent the interface region between the IGM and cold clouds that could be tentatively identified with protogalaxies. Since the IGM is in a thermally unstable state, the joint action of thermal conduction and radiative instabilities drives a *cooling wave* into the hot IGM. Thus, contrary to the common view in which thermal conduction should eventually lead to the evaporation and destruction of the cold phase, we argue that protogalaxies initiate the condensation process of gas which can be subsequently accreted by the galaxy itself. The relatively rarefied transition layer between the two phases represents a suitable environment for the formation of the Ly α forest forest absorption lines. Although very simple, the model is able to reproduce

most of the properties of Ly α forest clouds with a very restricted number of assumptions.

2. Conductive/Cooling Fronts

In this Section we describe briefly some results concerning conductive/cooling (CC) fronts following FS93 and Ferrara & Shchekinov (1996). We define a CC front as the interface between a hot and cold gas phase, whose structure is governed by the combined effects of thermal conduction and radiative cooling. As shown by FS93, dynamical effects (*i.e.*, shocks) can be important at the initial stages of the front evolution when the conductive timescale is shorter than the dynamical timescale of the system. However, after this transient the evolution relaxes to a quasi-isobaric regime. We will therefore consider only evolved stages for which pressure equilibrium holds approximately. For the same reason, we consider only "classical" Spitzer conductivity since saturation effects are important only in the initial evolutionary phases (FS93). We neglect magnetic fields, mostly because their existence and strength at high redshift are far from being established.

In the isobaric approximation, the hydrodynamic equations describing a CC front reduce to the energy equation, which could be cast in Lagrangian form as

$$\frac{\partial T}{\partial t} + c_p^{-1} \mathcal{L} - \frac{\partial}{\partial q} \left[\chi \frac{\partial T}{\partial q} \right] = 0, \quad (2.1)$$

where T is the gas temperature, \mathcal{L} is the net cooling rate per unit mass, c_p is the specific heat at constant pressure; $\chi = \kappa \rho / c_p$, where $\kappa = \eta T^{5/2}$ is the classical thermal conduction coefficient, is the reduced thermal conduction coefficient. The Lagrangian mass variable is

$$q = \int_{x_0}^x dx \rho(x, t)$$

where for all t the coordinate of a “reference” particle $x_0(t)$ is determined by the condition $v(x_0, t) = 0$. In eq. (2.1) lengths are normalized to the Field length (Field 1965) (Lagrangian formulation), $q_F = (\chi T c_p / \mathcal{L})^{1/2}$, and time to the cooling time $t_c = c_p T / \mathcal{L}$, both calculated for the hot medium.

The cooling function depends on the details of the microscopic processes responsible for the heating and cooling of the gas; for our purposes, however, it will be sufficient to consider a general form of \mathcal{L} reproducing a two phase medium with a cold stable, and a hot unstable equilibrium. This assumption closely resembles the IGM, supposedly constituted by cold clouds in pressure equilibrium with a surrounding, thermally unstable, hot diffuse gas. The simplest analytical function that retains such characteristics is $\mathcal{L}(T) = T(1 - T)$; the point $T = 1$ is thermally unstable, $(\partial \mathcal{L} / \partial T = -1)$, while $T = 0$ represents the thermally stable phase. In addition to the equilibrium points, this function also correctly mimicks the negative slope of the actual cooling function in the range $10^4 \text{ K} \lesssim T \lesssim 10^6 \text{ K}$.

Fig. 1 shows the temporal evolution of the CC front, as obtained from the numerical solution of eq. (2.1) with the above cooling function. Initially a cold cloud at $T = 0$ is immersed in the hot gas at $T = 1$. The evolution of the CC front induces a thermal wave in the cold medium and a cooling wave into the hot medium; the temperature profile is very steep due to the strong nonlinearity of the thermal conduction (shown by the enlarged view in Fig. 1). At about $t \simeq t_c$ the thermal wave propagation is inhibited by radiative losses (see FS93), and the cloud now acts as a finite perturbation for the unstable hot gas,

whose only possible fate is to condensate. As the CC front moves away from the origin, a cooling wave develops ($t \simeq 2t_c$); the profile of the wave becomes stationary and its shape corresponds to a quasi-linear thermal conductivity, in that $(\partial T/\partial q)^2 \ll |T(\partial^2 T/\partial q^2)|$. This fact suggests to compare the numerical results with an analytical travelling wave solution of eq. (2.1) obtained for linear conductivity ($\chi = \text{const.}$). Making the position $T(q, t) = T(\xi = q + 5Ut)$, substitution into eq. (2.1) yields the solution

$$T(\xi) = 1 - \frac{1}{(1 + e^{-U\xi})^2}, \quad (2.2)$$

where U is the propagation speed of the wave. In Fig. 1 we have fitted the curve of eq. (2.2) to the cooling wave, adjusting the parameter U to take into account that the exact solution is only quasi-linear; the agreement is remarkable for $U = 4/3 = \epsilon^{-1}$. Of course, it is not surprising that the value of U is close to unity, since it can be seen from dimensional analysis that it must be $U \sim q_F/t_c = 1$, in our units. The evolution depends rather weakly on the detailed shape of \mathcal{L} as long as an unstable point does exist. We will use this approximation to study the interface between Ly α forest clouds and the IGM in the next Section.

3. Conductive/cooling model for Ly α forest absorbers

To model Ly α forest clouds as cosmological CC fronts it is necessary to adopt a model for the IGM. Ikeuchi & Ostriker (1986) (and more recently Giroux & Shapiro 1995) have studied in detail the thermal history of the IGM from the era of the reheating to the present; they conclude that the most plausible scenario requires that both photoionization and bulk

mechanical heating (*i.e.*, shocks) contribute to the heating. The IGM reionization epoch is still uncertain, but the limits on the Gunn-Peterson effect (Webb *et al.* 1992) suggest that it must have occurred at $z \geq 5$. Ikeuchi & Ostriker show that, if the reionization occurred at $z = 10$ - for example - the IGM entered the adiabatic expansion phase already at $z \simeq 4$. Since we will mostly concentrate on the $z \lesssim 4$ epoch, we will assume in what follows that the IGM is adiabatic, and therefore temperature and pressure are $T(z) = T_0(1+z)^2$, $p(z) = p_0(1+z)^5$; the local values are $T_0 = 3 \times 10^4$ K and $p_0 = 3 \times 10^{-2}$ cm $^{-3}$ K; we use the cosmology $\Omega = 1$ and $h_{100} = 0.5$; in addition $\Omega_b = 0.03$.

Since the heat transport relies on the presence of a hot IGM, it is likely that CC fronts were generated immediately after the reionization epoch. Next, they propagate away from the cloud with velocity decreasing rapidly with redshift: $U \simeq q_F/t_c \propto (1+z)^6$, assuming that IGM cooling is dominated at early epochs by inverse Compton scattering on the microwave background. A stationary cooling wave profile, similar to the one given in eq. (2.2), will form after a few cooling times, as demonstrated in Fig. 1; this requires that the Hubble time is larger than t_c , a condition satisfied for $z \gtrsim 4$. If reionization occurred at $z = 10$, the distance travelled by the cooling wave at $z = 4$ is $d = (m_H H_0)^{-1} \int_4^{10} dz (1+z)^{-5/2} U n^{-1} = 60$ kpc; the cool material behind the wave is accreted by the parent protogalaxy at a rate $\dot{M}_{in} \sim m_H n d^3 t_{H,4}^{-1} = 5 \times 10^7$ M $_{\odot}$ Gyr $^{-1}$, where $t_{H,4}$ is the Hubble time at $z = 4$. As the front has reached the steady-state, its width (of the order of q_F) is regulated only by the changes of the IGM parameters due to Hubble expansion; since $q_F \propto (1+z)^2$, the front shrinks as z decreases (it can be shown that the interface reacts almost instantaneously to external changes).

The neutral hydrogen column density of the Ly α forest cloud, N_{HI} , will be in general a function both of the impact parameter, b , at which the interface is intersected by the line of sight and of redshift. Assuming spherical symmetry, with radial coordinate $r(q)$, the expression for N_{HI} is

$$N_{HI}(b, z) = \frac{2}{m_H} \int_{q(b)}^{\epsilon q_F} dq \{1 - x[T(q, z), n(q, z)]\} \frac{r(q)}{\sqrt{r^2(q) - b^2}}. \quad (3.1)$$

The hydrogen ionization fraction x has been derived under the assumption of ionization equilibrium due to photo- and collisional ionizations and that the time variation of the diffuse UV flux is $J(z) = 10^{-21}[(1+z)/3.5]^2 \text{ ergs cm}^{-2} \text{ s}^{-1} \text{ Hz}^{-1} \text{ sr}^{-1}$. The temperature profile follows from eq. (2.2) and $n(q) = p/kT(q)$; we have neglected geometrical corrections in the solution $T(q)$ due to spherical geometry. The lower integration limit is the Lagrangian impact parameter implicitly defined by $m_H^{-1} \int_0^{q(b)} dq/n(q) = b - d$, while the upper limit is the characteristic size of the interface. The size of the central cold core is determined by the distance $d \simeq 60 \text{ kpc}$ travelled by the front in the early stages of evolution; however, the value of the integral depends very weakly on any reasonable choice for d . A sketch of the geometry is given in Fig. 2. Impact parameters $b \leq d$ are not considered because of the negligible contribution of the Ly α forest cloud to the central damped Ly α system.

Fig. 3 shows the curves for N_{HI} from eq. (3.1) as a function of $q(b)$ for different redshifts. Therefore, $q(b) = 0$ corresponds in physical units to an impact parameter $b = d$ and $q(b) = 1$ corresponds to $b = \epsilon \ell_F + d$, where $\ell_F = q_F/m_H n$ is the Field length in physical units; ℓ_F depends on redshift as

$$\ell_F = \left(\frac{\chi T c_p}{\mathcal{L} \rho^2} \right)^{1/2} = 333 (1+z)^{-1} \text{ kpc}, \quad (3.2)$$

for the adopted IGM parameters.

The hydrogen column density is a rather flat function of $q(b)$ for values $q(b) \leq 0.1$, *i.e.*, close to the central cold cloud, and decreases roughly as $q(b)^{-4}$ for $z = 4$ and less steeply for smaller values of z . The values of N_{HI} are in the range $10^{12} - 3 \times 10^{16} \text{ cm}^{-2}$ for $0 \leq z \leq 4$. An useful analytical approximation to the curves shown in Fig. 3 between $z = 0$ and $z = 3$ is

$$N_{HI}(q) = N_{HI}^0 \left[\frac{(1+z)^5}{1 + \left(\frac{q}{a}\right)^{1+z}} \right], \quad (3.3)$$

with $N_{HI}^0 = 7 \times 10^{12} \text{ cm}^{-2}$, and $a = 0.1$.

4. Implications

In the present model N_{HI} is a function both of redshift and of the impact parameter for the cloud: it decreases with decreasing z and with increasing b ; the variation range is $10^{12} \text{ cm}^{-2} \lesssim N_{HI} \lesssim 3 \times 10^{16} \text{ cm}^{-2}$ for $0 < z < 4$. Therefore, below $N_{HI} = 10^{12}$ we expect a turnoff in the distribution of the clouds; this prediction awaits an observational test from oncoming high sensitivity observations with the Keck telescope.

The temperature is a function of the depth inside the cloud along the line of sight (see Fig. 2), with radial dependence as described by eq.(2.2). Its range is bracketed by the temperature of the cold cloud (here assumed to be $T_c = 10^4 \text{ K}$) and the temperature of the IGM, $T(z)$ (roughly $10^5 - 7 \times 10^5 \text{ K}$). For a given Ly α forest cloud, the temperature

is anticorrelated with N_{HI} , since the inner regions are colder than the external ones. However, since this cold material is far from hydrostatic equilibrium in the gravitational field of the parent protogalaxy, it will be accelerated towards the center acquiring bulk velocity that could reverse the sign of the $T - N_{HI}$ correlation. This conclusion must be substantiated by fully hydrodynamical calculations.

An interesting feature of the model is the presence of a natural scale for the size of the clouds, the Field length ℓ_F (eq. [3.2]). Thus, the size of Ly α forest clouds is constrained directly by physical arguments. For the adopted model of the IGM, typical transverse sizes are ~ 50 kpc and ~ 150 kpc, for $z = 4$ and $z = 1$, respectively. Hence, for a constant number of absorbers per comoving volume, the probability to detect a Ly α forest cloud in a quasar pair should be higher at low redshifts *if the signal-to-noise ratio were infinite* (see below).

The expected redshift distribution of absorbers can be calculated as follows. The number of absorbers between z and $z + dz$ is

$$dN = N_a c dt \int_0^{b_m} db 2\pi b = \frac{\pi N_0 c}{H_0} (1+z)^{1/2} b_m^2 dz, \quad (4.1),$$

where $N_a = N_0(1+z)^3$ is the density of absorbers. The maximum impact parameter, b_m , is determined by the observational threshold for detection of Ly α forest absorption: $b_m = b(N_{HI}^{th})$. For example, from Fig. 3, at $z = 3$ and for $N_{HI}^{th} = 10^{13} \text{ cm}^{-2}$, which represents a typical threshold for current observations, the maximum value of $q(b)$ sampled is ~ 0.4 (there is an almost linear relation between $q(b)$ and b). For the previous value of N_{HI}^{th} , a fit to the numerical results gives $b_m \propto \ell_F (1+z)^\alpha$. In $1 \leq z \leq 4$ the best fit value

is $\alpha = 1.4$. For a higher value of N_{HI}^{th} , the corresponding value of α increases, *i.e.*, the distribution becomes steeper. Upon substitution in eq. (4.1), with $\alpha = 1.4$, we obtain $dN/dz \propto (1+z)^{1.3}$.

The index of the distribution is slightly smaller than the one found by Bechtold (1994) ($\gamma = 1.32 \pm 0.24$) for a sample of lines complete to equivalent width $W_{th} = 0.16 \text{ \AA}$. According to her curves of growth, depending on the adopted Doppler parameter, this corresponds to $6 \times 10^{13} \text{ cm}^{-2} \lesssim N_{HI} \lesssim 10^{14} \text{ cm}^{-2}$, about an order of magnitude larger than N_{HI}^{th} . Since Bechtold has also noted a decreasing trend for γ with decreasing W_{th} , it is reasonable to expect that for lower W_{th} the distribution flattens to a value similar to the one we have found. However, this physical effect can be difficult to disentangle from spurious line blending effects (Trevese *et al.* 1992).

The column density distribution for the absorbers is

$$\frac{dN}{dN_{HI}} = 2\pi N_0 \int_0^{z_m} dz b(N_{HI}, z) \frac{db}{dq}(N_{HI}, z) \frac{dq}{dN_{HI}}(N_{HI}, z) (1+z)^3 \frac{dt}{dz}. \quad (4.2)$$

Using the definition of the Lagrangian coordinate q to eliminate b and eq. (3.3) to eliminate q , we get $dN/dN_{HI} \propto N_{HI}^{-2} f(N_{HI}, z_m)$.

Numerical integration shows that the function $f(N_{HI}, z_m)$ depends very weakly on N_{HI} and can be approximated by a power-law with index -0.1 . Therefore, from eq. (4.3) we find that the column density distribution for the Ly α forest clouds is also a power-law with index $\beta = -2.1$. The value of β is independent of z_m and somewhat higher than the one ($\beta = -1.4$) obtained by Dobrzycki & Bechtold (1996).

Two additional consequences of our model can be outlined: i) Ly α forest clouds should

be quite often associated with damped Ly α clouds, from which they are originated, at least at high z . At low z , damped Ly α systems can be destroyed by violent episodes of star formation (Salpeter 1995) and isolated “fossile” Ly α forest clouds remain; ii) metals abundances at the level detected by Tytler (1995) could be easily reproduced by our model if part of the Ly α forest gas is coming from a metal-rich protogalaxy, or if the IGM is polluted by metals associated with the same blast waves responsible for its bulk heating.

Acknowledgments

It is a pleasure to thank E. Giallongo, P. Shapiro and particularly D. Bowen for stimulating discussions. Yu.S. acknowledges the hospitality of the Osservatorio Astrofisico di Arcetri and the partial support from ESO grant B-06-013 and Russian Foundation for Basic Research grant 94-02-05016-a.

References

- Bechtold, J. 1994, ApJS, 91, 1
- Bechtold, J., Crotts, A. P. S., Duncan, R. C. & Fang, Y. 1994, ApJ, 437, L83
- Carswell, R. F., Lanzetta, K. M., Parnell, H. C., & Webb, J. K. 1991, ApJ, 371, 36
- Dinshaw, N., Impey, C. D., Foltz, C. B., Weymann, R. J. & Chaffee, F. H. 1994, 437, L87
- Dobrzycki, A. & Bechtold, J. 1996, ApJ, 457, 102
- Ferrara, A. & Shchekinov, Yu. 1993, ApJ, 417, 595 (FS93)
- Ferrara, A. & Shchekinov, Yu. 1996, MNRAS, submitted
- Field, G. B. 1965, ApJ, 142, 531
- Giallongo, E., Cristiani, S., Fontana, A. & Trevese, D. 1993, ApJ, 416, 137
- Giroux, M. & Shapiro, P. R. 1995, ApJS, in press
- Ikeuchi, S. & Ostriker, J. P. 1986, ApJ, 301, 522
- Pettini, M., Hunstead, R. W., Smith, L. J. & Mar, D. P. 1990, MNRAS, 246, 545
- Rauch, M., Carswell, R. F., Webb, J. K., & Weymann, R. J. 1993, MNRAS, 260, 589
- Salpeter, E. E. 1995, in The Physics of the Interstellar and Intergalactic Medium, PASP Series, Vol. 80, eds. A. Ferrara, C. F. McKee, C. Heiles, P. R. Shapiro, (PASP: San Francisco), in press
- Trevese, D. Giallongo, E. & Camurani, L. 1992, ApJ, 398, 491

Tytler, D. 1995, in “Proceedings of the ESO QSO Absorption Line Workshop”, in press

Webb, J. K., Barcons, X., Carswell, R. F. & Parnell, H. C. 1992, MNRAS, 255, 319

Figure 1 Evolution of the structure of a conductive/cooling front; time is in units of the cooling time, t_c , in the hot gas; temperature is normalized to the temperature in the hot gas. Solid curves refer to (from right to left) $t = 0, 0.5, 1, 2, 3, 10$; the dotted curve shows the analytical approximation for $t = 10$. The inner panel shows an enlargement of the region close to the origin.

Figure 2 Sketch of the geometry used for the conductive/cooling model.

Figure 3 Distribution of the hydrogen column density for a Ly α forest cloud as a function of the Lagrangian impact parameter $q(b)$ (see text) for different redshifts $z = 4, 3, 2, 1, 0$ from the uppermost to lowest curves; $q(b)$ is in units of the Lagrangian Field length at the relevant redshift.

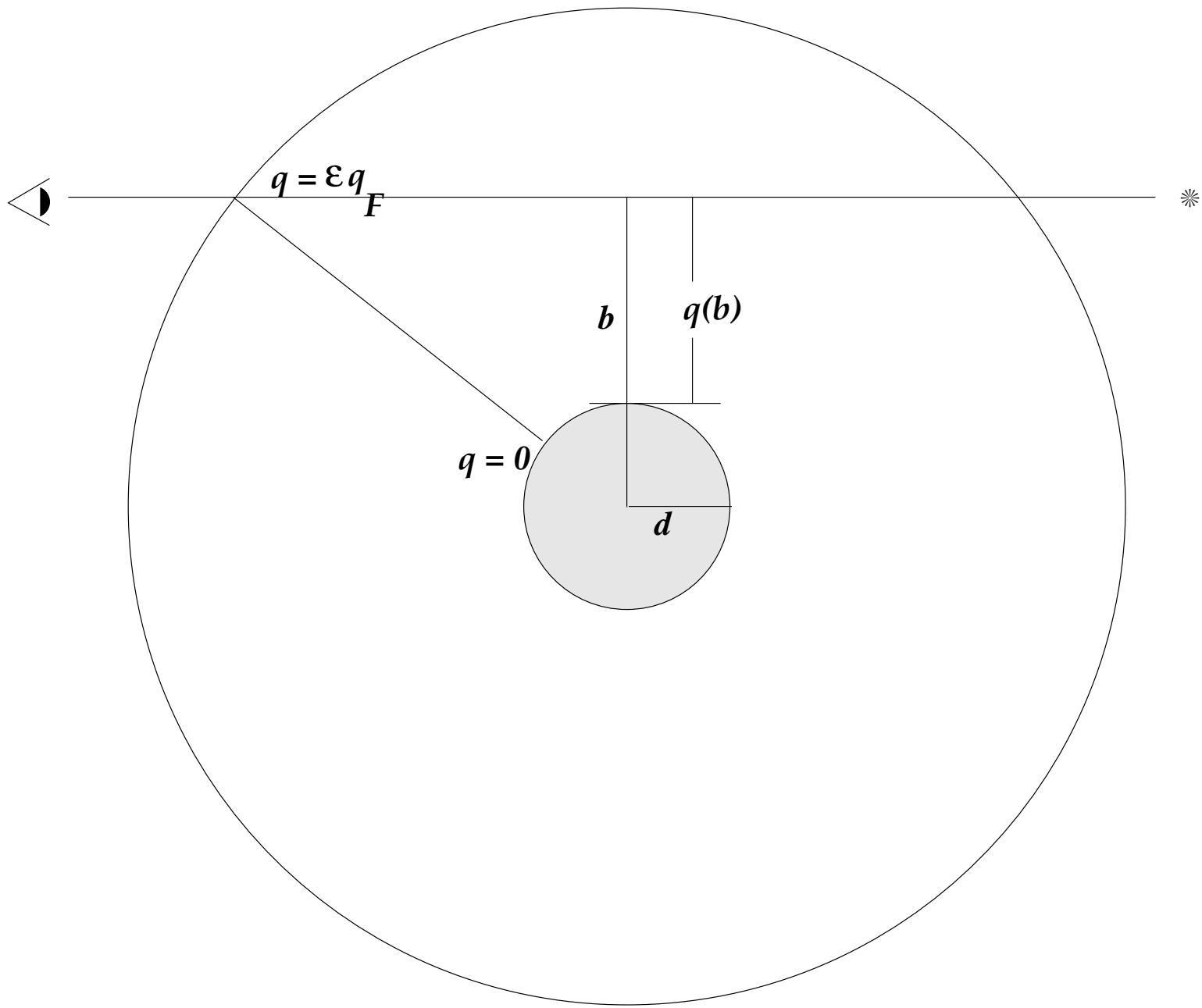


Figure 2

